Journal of Multidisciplinary Engineering Science Studies (JMESS)
ISSN: 2458-925X
Vol. 2 Issue 11, November - 2016

Maximum Heat Transfer Density From Finned Tubes Cooled By Natural Convection

Ahmed Waheed Mustafa[1] Mays Munir Ismael[2]
AL-Nahrain University College of Engineering Mechanical Engineering Department
ahmedwah@eng.nahrainuniv.edu.iq[1], maymunir336@yahoo.com[2]

***Abstract*—The optimal spacing between finned tubes cooled by free convection is studied numerically. A row of isothermal finned tubes are installed in a fixed volume and the spacing between them is selected according to the constructal theory (Bejan's theory). In this theory the spacing between the tubes is chosen such that the heat transfer density is maximized. A finite volume method is employed to solve the governing equations; SIMPLE algorithm with collocated grid is utilized for coupling between velocity and pressure. For the numerical results, the range of Rayleigh number is ($10^3 \le Ra \le 10^5$), the range of the tube position is ($0.25 \le \delta \le 0.75$), and the working fluid is air (Pr =0.71). Experimental study is also carried out in order to demonstrate the existence of the optimal spacing. The experimental Rayleigh number is ($Ra = 3.8 \times 10^4$) and the tube position of the finned tube is (0.667) .The numerical results show that the optimal spacing decreases as Rayleigh number increases for all tube positions, and the maximum density of heat transfer increases as the Raleigh number increases for all tube positions and for $Ra=10^5$ the highest value of heat transfer density occurs at tube position (δ =0.75) while the lowest value occurs at tube position (δ =0.25). The results also show that the optimal spacing remains constant with change of the tube position at constant Rayleigh number, and the agreement between the experimental and numerical heat transfer density is qualitative.**

Keywords—Constructal theory, optimal spacing, finned tubes, natural convection

Nomenclature

b Position of the tube (m)
d diameter of the tube (m)
D Non-dimensional diameter of the tube
g Gravity acceleration (m/s^2)
h Total height of fin and tube (m)
H_d Dimensionless downstream extension
H_u Dimensionless upstream extension
k Thermal conductivity (W/m.k)
L Total length of the domain (m)
L_f Fin length (m)
p Pressure (N/m^2)
P Non-dimensional pressure
Pr Prandtl number
q Heat transfer rate (W)
Q Dimensionless heat transfer density
Ra Rayleigh number
s Spacing between the tubes (m)
S Dimensionless Spacing
t Temperature (^{o}C)
T Dimensionless temperature
T_w Wall temperature (^{o}C)
T_∞ Ambient temperature (^{o}C)
u Horizontal velocity (m/s)
U Dimensionless horizontal velocity
v Vertical velocity (m/s)
V Dimensionless vertical velocity
V Volume (m^3)
w Width (m)
x Horizontal Coordinate (m)
X Dimensionless Horizontal Coordinate
y Vertical coordinate (m)
Y Dimensionless vertical coordinate

Greek Symbols

α Thermal diffusivity (m^2/s)
β Coefficient of thermal expansion (K^{-1})
δ Dimensionless position of tube
ρ Density (Kg/m^3)
ν Kinematic viscosity (Pa.s)

Subscripts

Max Maximum value
Opt Optimum value

1. Introduction

In heat transfer, constructal theory (Bejan's theory) is used to generate the flow configuration by optimizing the heat transfer density under (space) volume constraint. Constructal theory states that the flow configuration is free to morph in the follow-up of maximal global performance (objective function) under global constraints, Bejan A. and Lorente S., (2008), [1]. By depending on constructal theory, the optimal spacing between plates and cylinders cooled by natural convection can be found, in each geometry, the total volume is fixed and the objective is to maximize the overall thermal conductance between the tubes. Bejan A., (1984), [2] found the optimal spacing between vertical plates installed in a fixed volume by using the intersecting of asymptotes method. The study was employed for isothermal vertical plates cooled by natural convection. He found that the optimal spacing was proportional to the Rayliegh number to the power of (-1/4). Bejan A. et al. (1995), [3] carried out a numerical and experimental study of how to choose the spacing among horizontal cylinders installed in a fixed volume cooled by laminar free convection. They maximized the total density of heat transfer between the assembly and the ambient. The Numerical and experimental simulations cover the Rayleigh number range of $10^4 \le Ra \le 10^7$and Pr = 0.72. Ledezma G. A. and Bejan A., (1997), [4] investigated numerically and experimentally the free convection from staggered vertical plates installed in fixed space. They maximized the density of heat transfer and they considered three degrees of freedom; the horizontal spacing between adjacent columns, the stagger between columns and the plate dimensions. Numerical and experimental simulations cover the Rayleigh number range of $10^3 \le Ra \le 10^6$, and the working fluid was air with Pr=0.72. The conclusion demonstrated numerically and experimentally that it was possible to optimize geometrically the internal architecture of a fixed volume such that its global thermal resistance was minimized. Da Silva and A. Bejan,(2004),[5] studied numerically the free convection in vertical converging or diverging channel with optimized for density of heat transfer. They considered three degrees of freedom: the distribution of heat on the wall, wall to wall spacing, and the angle between the two walls. The optimization was performed in the range of $10^5 \le Ra \le 10^7$and Pr=0.7. The walls were partially heated either at top of the channel or at the bottom of the channel. They proved that the density of heat transfer increased by putting the unheated part at the upper sections. They also showed that the best angle among the walls was almost zero when Ra number was high. Da Silva A. K. and Bejan A., (2005), [6] designed numerically a multi-scale plates geometry cooled by free convection by using constructal theory. They maximized the density of heat transfer rate. They put small plates in the unused heat transfer area between the large plates. They used finite element method to discretize the governing equation in the range of Rayleigh number of $10^5 \le Ra \le 10^8$, and Pr= 0.7. They showed that the density of heat transfer increased by putting the small plates between the large plates. Da Silva A.K. et al. (2005), [7] studied the free convection from discrete heat sources placed in vertical open channel with the constructal theory. They considered two cases, the first was single heat source under variable size, and the second was heat sources with fixed size. They applied the constructal theory to maximize the thermal conductance between the cold air and the discrete heat sources or to minimize the hot spot on the hot sources. Rayleigh number was in the range of ($10^2 \le Ra \le 10^4$) and Pr = 0.7. They showed that for case one the thermal performance can be maximized as the heat source not covering the entire wall at Ra =10^2 and 10^3. Bello-Ochende T. and Bejan A., (2005), [8] designed numerically a multi-scale cylinders geometry cooled by free convection by using constructal theory. They maximized the density of heat transfer rate. They put small cylinders in the unused heat transfer area between the large cylinders. They used finite element method to discretize the governing equation in the range of Rayleigh number of $10^5 \le Ra \le 10^8$, and Pr= 0.7. They showed that the density of heat transfer increased by putting the small cylinders between the large cylinders. Page L. et al., (2011), [9] investigated numerically the free convection from single scale rotating cylinders. They used the constructal theory to maximize the density of heat transfer rate. The range of Rayleigh number was ($10^1 \le Ra \le 10^4$), the range of rotating speed was ($0 \le \tilde{\omega}_o \le 10$), and the fluid was air (Pr=0.7). They found that the optimized spacing decreases as Rayleigh number increases and the heat transfer density increases. Page L. et al. (2013), [10] investigated numerically the free convection from multi-scales rotating cylinders. They used constructal theory in order to find the optimal arrangement of the geometry. The range of Rayleigh number was ($10^2 \le Ra \le 10^4$), the range of rotating speed was ($0 \le \tilde{\omega}_o \le 10$), and the fluid was air (Pr=0.7). Small cylinders were put in the unused regions of heat transfer. They found that there were no effects of the rotating cylinders on heat transfer density in compare with the stationary cylinders except at high speeds of rotation. It is obvious from the literature that there is no attempt to find the optimal spacing between finned tubes cooled by free convection with constructal theory, so that the present study uses the constructal theory to find the optimal spacing numerically.

2. Mathematical Model

Consider a row of finned tubes installed in a fixed volume per unit depth (*h L*) as shown in figure (1). Longitudinal fins are attached to the tubes and the total height of the tube and fin is (h), the diameter of the tubes is half of the total height (*d*=*h*/2). Three different vertical positions of the tube with respect to the fin (*b*) are considered as (*b*=0.25*h*, 0.5*h*, and 0.75*h*). Fin thickness is negligible in compare with the diameter of the tube. The position of the tube as a ratio is defined as ($\delta = b/h$). The tubes and the fins are maintained at constant wall (hot) temperature of (T_w), and the ambient temperature is maintained at constant temperature of (T_∞). The objective is to find the number of tubes or the tube – to – tube spacing (*s*) for different tube positions (δ) in order to maximize the density of heat transfer. In this geometry there are two degrees of freedom, the first is the spacing between the tubes (*s*) and the second is the tube position (δ). The dimensionless governing equations for steady, laminar, two dimensional and incompressible flow with Boussinesq approximation for the density in the buoyancy term can be written as; Zhang Z. et al. (1991), [11]

$$\frac{\partial U}{\partial X} + \frac{\partial V}{\partial Y} = 0 \quad (1)$$

$$\left(U\frac{\partial U}{\partial X} + V\frac{\partial U}{\partial Y}\right) = -\frac{\partial P}{\partial X} + \left(\frac{Pr}{Ra}\right)^{1/2}\left(\frac{\partial^2 U}{\partial X^2} + \frac{\partial^2 U}{\partial Y^2}\right) \quad (2)$$

$$\left(U\frac{\partial V}{\partial X} + V\frac{\partial V}{\partial Y}\right) = -\frac{\partial P}{\partial X} + \left(\frac{Pr}{Ra}\right)^{1/2}\left(\frac{\partial^2 V}{\partial X^2} + \frac{\partial^2 V}{\partial Y^2}\right) + T \quad (3)$$

$$\left(U\frac{\partial T}{\partial X} + V\frac{\partial T}{\partial Y}\right) = \frac{1}{(Ra\,Pr)^{\frac{1}{2}}}\left(\frac{\partial^2 T}{\partial X^2} + \frac{\partial^2 T}{\partial Y^2}\right) \quad (4)$$

The non-dimensional variables and groups used are;

$$X=\frac{x}{h},Y=\frac{y}{h},U=\frac{u}{\left(\frac{\propto}{h}\right)(Ra\ Pr)^{\frac{1}{2}}},$$

$$V=\frac{v}{(\frac{\propto}{h})\ (Ra\ Pr)^{\frac{1}{2}}},P=\frac{Pd^{2}}{\propto^{2}\ \rho\ Ra\ Pr},T=\frac{t-T_{\infty}}{T_{w}-T_{\infty}},Pr$$

$$=\frac{v}{\propto},Ra=\frac{g\,\beta h^{3}\ (T_{w}-T_{\infty})}{\propto\ v}\ (5)$$

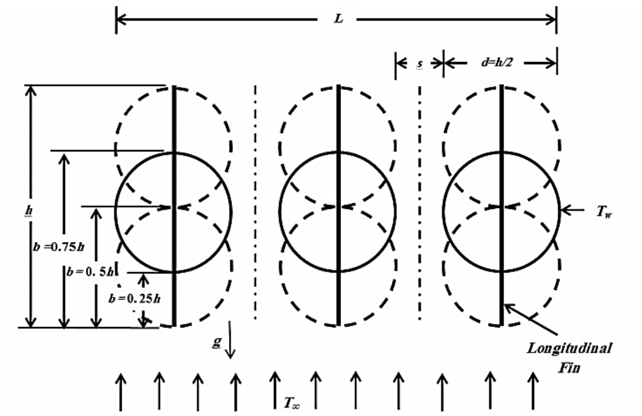

Figure (1) Physical Geometry of the Present Problem

Since the flow is symmetrical between the tubes, only half of the flow channel between two tubes can be used to find the spacing in the numerical solution. Half of the flow channel is shown in figure (2). The total height of the channel is (H_u+H+ H_d), the upstream height (H_u) and downstream (H_d) are added to avoid the applying of incorrect velocity and temperature at the inlet and outlet of the channel, these extension (H_u, H_d) are selected according to accuracy tests as shown later.

The flow and thermal dimensionless boundary conditions on the half channel are shown in figure (2) and can be summarized as;

<u>Tube and fin surfaces</u> ($0\le Y\le H$) (no slip and no penetration and constant wall temperature $U=V=0\,,T=1$)

<u>Channel inlet</u> $\left(0\le X\le\left(\frac{S+D}{2}\right)\right)\ \left(U=\frac{\partial V}{\partial Y}=0\,,T=0\,,P=0\right)$

<u>Channel exit</u> $\left(0\le X\le\left(\frac{S+D}{2}\right)\right)\left(\frac{\partial(U,V,T)}{\partial Y}=0\,,P=0\right)$

<u>Left and right sides of the upstream section</u> ($-H_u\le Y\le 0$) (free slip and no penetration $U=\frac{\partial V}{\partial X}=0\,,\frac{\partial P}{\partial X}=0\,,\frac{\partial T}{\partial X}=0$)

<u>Left side of the downstream section</u> ($H\le Y\le H+H_d$) (free slip and no penetration $U=\frac{\partial V}{\partial X}=0\,,\frac{\partial P}{\partial X}=0\,,\frac{\partial T}{\partial X}=0$)

<u>Right side of the downstream section</u> ($H\le Y\le H+H_d$) (zero stress $\frac{\partial(V,U)}{\partial X}=0,\frac{\partial P}{\partial X}=0\,,\frac{\partial T}{\partial X}=0$)

The right side of the downstream boundary condition is applied to permit fluid to enter the domain horizontally in order to avoid the vertical acceleration which generated by chimney effects, Bello-Ochende T. and Bejan A.,(2005), [8].

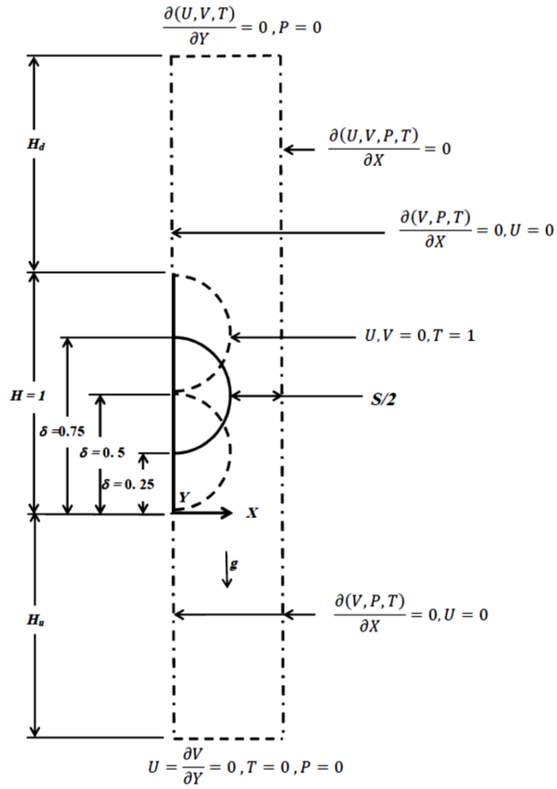

Figure (2) Dimensionless Boundary Conditions on the Flow Channel

3. Optimization of Heat Transfer (Maximum Heat Transfer Density) Based on Constructal Theory

The spacing between the tubes is to be chosen such that the heat transfer density (objective function) is maximized. The heat transfer density is the heat transfer rate per unit volume and given as;

$$q'''=\frac{q}{V}=\frac{q}{(s+d)hw}=\frac{q'}{(s+d)h}\ (6)$$

Where q′ = Total heat transfer rate from one tube per unit width.

The heat transfer density can be written in non-dimensional form as;

$$Q=\frac{q\prime\,h^{2}}{k\,(T_{w}-T_{\infty})(s+d)h}\ (7)$$

$$Q\ =\frac{-\left(\int_{0}^{h}k\frac{\partial t}{\partial x}\,dy\right)h}{k(T_{w}-T_{\infty})(s+d)}=\frac{-\int_{0}^{1}\frac{\partial T}{\partial X}\,dY}{(S+0.5)}\ (8)$$

The objective function (heat transfer density) subjected to the constraint that the total volume per unit width is fixed. (This is based on constructal law)

∴ ($h\ L$) = Constant (9)

4. Experimental Apparatus:

In order to find the optimal spacing between finned tubes experimentally a rows of heated finned tubes are installed in a fixed volume. Figure (3) shows the main parts of the rows used in the experiments. In all experiments the tubes are placed is fixed volume of (*H*=27 mm, *L*=150 mm, and *w*=102 mm), these dimensions are chosen according to, Bejan et al. (1995). In order to ensure 2D flow and laminar Rayleigh number. Three rows of finned tubes are manufactured from circular copper tubes and copper plates for the experiments, the first row consists of 5 tubes, the second row consists of 4 tubes, and the third row consists of 3 tubes. The spacing between the tubes in the first row is (2.7 mm) which corresponds to (S=s/l= 0.11), the spacing between the tubes in the second row is (10 mm) which corresponds to (S=s/l=0.37), and the spacing between the tubes in the third row is (24 mm) which corresponds to (S=s/l=0.88). The three assemblies of tubes are shown in plate (1). In order to minimize the heat loss from the tube ends, the tubes are held between two vertical wooden walls as shown in plate (1)**,** Bejan et al. (1995). The assembly is placed in open top and bottom ends Perspex enclosure of height (1m) and cross section of (0.42m x 0.42m), to minimize the radiation losses the walls of the enclosure are covered with aluminum foils as shown in plate (2). Each cylinder has fixed dimensions (D= 18 mm and L= 170 mm) and welded with a plate fin (L_f= 9 mm and L= 170 mm), the soldering material which used to join cylinders with the fin plates are made from the same material (copper). In all experiment the fin is attached on the bottom of tube with tube position (δ= 0.667) (fin to tube diameter ratio is 0.5).

To heat the tubes a cartridge heaters of 12 mm diameter and 300 Watts are installed inside the tubes. These heaters are placed concentrically inside the tubes by using two rings at each ends of the tubes, Bejan et al. (1995). The gaps between the heaters and the tubes are filled with the magnesium oxide powder. The heaters are connected in parallel and supplied by variable transformer which used to control the electrical power**,** Bejan et al. (1995). The current and the voltage are measured by using (Digital Clamp Meter UNI-T UT200A with accuracy $\pm$(1.5% +5)) .The uniform in temperature on the tube wall is firstly checked by six T-type thermocouples (calibrated with a mixture of ice and water) which located on the positions shown in figure (4). The tube is then rotated to change the position of the thermocouples, Bejan et al. (1995). The temperature is practically uniform when the maximum difference in the six locations about (0.3°C). The temperatures (T_{w1}) and (T_{w2}) are measured in the mid-plane of the row in the locations shown in figure (5), as steady state is attained the maximum temperature registered is (T_{w1}) which used in the calculation of heat transfer density as shown later.

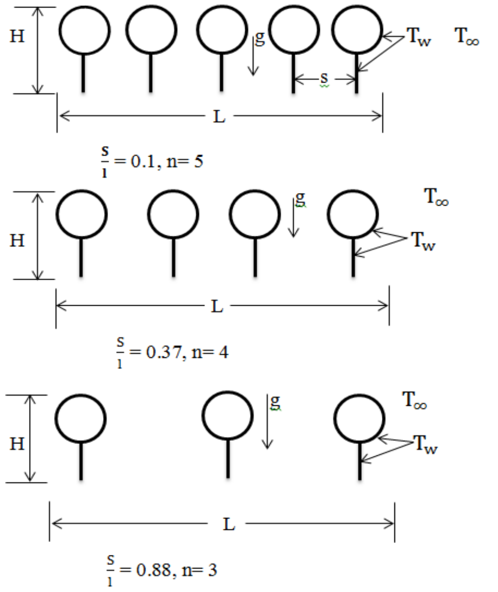

Figure (3) Details of the main parts of the rows used in the Experimental Apparatus

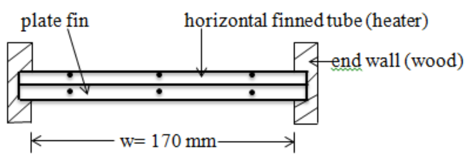

Figure (4) Position of the thermocouples on the finned tubes

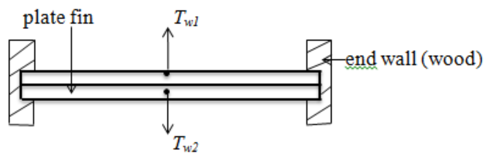

Figure (5) Position of the thermocouples for (T_{w1}) and (T_{w2}) used in calculating heat transfer density.

s/l = 0.11

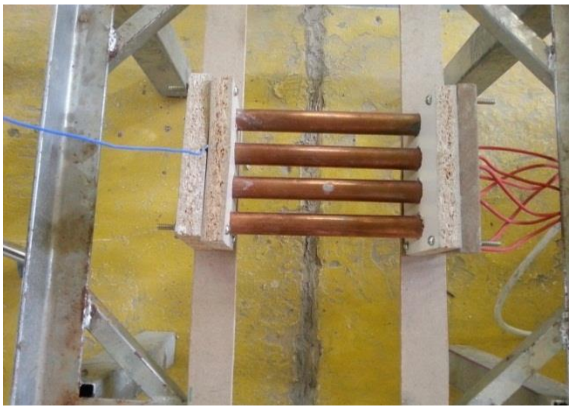

s/l = 0.37

s/l = 0.88

Plate (1) Rows of Heated Finned Tubes

Plate (2) Enclosure

5. Experimental Procedure and Calculations:

The first run (experiment for the row of 5 tubes) is started by supplying the electric power to the heaters to heat the finned tube. After the steady state attained which takes about 6-8 hours, the temperatures (T_{w1}, T_{w2} T_{∞}), the current, and the voltage are recorded. The steady state is attained when the percentage change in T_w, voltage, and current is less than 0.6%, 0.2% and 0.2% respectively.

The second experiment (4 tubes) and the third experiment (3 tubes) are conducted by adjusting the current in order to obtain the same temperature of the first experiment (T_{w1}) to make all the three experiments conducted at the same Rayleigh number.

6. Numerical Procedure, Grid Independence Test, and Validation

A FORTRAN program is written to solve the algebraic equations which obtained by the finite volume method. The general transport equation is firstly transformed to curvilinear coordinates and the convective term is discretized by hybrid scheme while the diffusion term is discretized by second order central scheme. For coupling between the pressure and velocity SIMPLE algorithm is employed. To prevent the oscillation in the pressure field the interpolation method of Rhie, C. M., and Chow, W. L., (1983), [12], is used. The solution algorithm can be summarized as;

1- Solve the discretized momentum equations to find the velocity field.

2- Solve the pressure correction equation to find the corrected pressure.

3- Correct the velocity field by using the corrected pressure.

4- Solve the discretized energy equation to find the temperature.

5- Repeat the steps (1-4) until convergence attained.

6- Find the heat transfer density from equation 8.

The grid independence test is performed for three grids for configuration at which (Ra = 10^4, δ =0.25, and S = 0.3). The grid independence test showed that the increasing of the grid size decreases the error percentage, and the minimum error occurs at 50×50 control volumes per (H). So this grid size is used and adopted in all the numerical results. Gird independence test is illustrated in table (1). A generated grid for control volumes of (175x50) in the whole domain is illustrated in figure (6). To apply the correct velocity and temperature at the inlet and outlet of the channel, the upstream extension (H_u) is added at the inlet of the channel and downstream extension (H_d) is added at the outlet of the channel. It is observed from the table (2) for (Ra = 10^5, δ=0.75, and S = 0.2) that the increasing in downstream extension to (H_d =3.5) and keeping the upstream at (H_u =0.5) leads to reduce the error in the heat transfer density to 1.4%. Based on this test the value of (H_u=0.5) and (H_d =3.5) have been depended in all numerical results.The numerical results are validated by comparing the results of (S_{opt}) with the numerical results of Da Silva and Bejan,(2004), [6] for natural convection between vertical isothermal plates and with Bello-Ochende and Bejan, (2005), [8] for natural convection between isothermal cylinders. Both comparisons are carried out at (Ra =10^5). Good agreement can be shown in table (3) for both cases.

Table 1 Grid Independence Test for the Case (Ra = 10^4, δ=0.25, and S=0.3)

Number of Control Volumes Per H	Q	Error%
30 x 30	13.925020	---------
40 x40	14.071420	1.04
50 x 50	14.149130	0.554

Table 2 Downstream Extension Test for the Case (Ra = 10^5, δ=0.75, H_u =0.5 and S=0.2)

H_d	Q	Error %
2	23.406150	----------
2.5	23.877630	1.9
3	24.271650	1.6
3.5	24.630340	1.4

Flat Plate	
Da Silva A.K., and Bejan A., (2004) [6]	Present
0.129	0.13
Circular Tube	
Bello- Ochende T., and Bejan A., (2005) [8]	Present
0.104	0.12

Table 3 Comparison of the Numerical Results for (S_{opt}) with the Previous Results for Case Ra =10^5 for flat plate and circular tube.

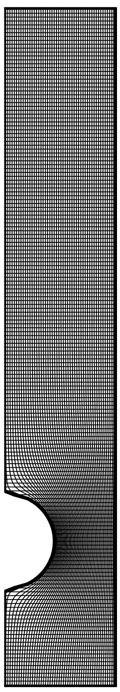

Figure (6) Generated Grid for CVs (175X50)

7. Results and Discussion

The numerical results are presented in this section for, temperature contours, optimal spacing, and density of heat transfer for different values of tube position (0.25 ≤ δ ≤ 0.75)**.** The range of Rayleigh number is ($10^3 \leq Ra \leq 10^5$) and the working fluid is air with (Pr =0.71).

Figure (7) shows the temperature contour as a function of the spacing between the tubes (S) for (Ra =10^3) and tube position (δ = 0.25). For small spacing (S < 0.25) the downstream region is occupied by hot fluid at temperature same as the wall temperature (red region), this is due to that the small spacing between the tubes prevents the cold air to flow downstream and the air there still hot (overworked fluid). As the spacing between the tubes increases (S > 0.25) the downstream temperature begins to decrease and become less than the wall temperature and this is clear from the appearance of the (orange, yellow and green) regions. At some spacing the thermal boundary layers from both sides are merged at the downstream region (the channel is fitted with the convective flow body) , at this spacing the heat transfer density becomes maximum and the spacing represents the optimal spacing, in this case (S_{opt} = 0.35). Further increasing in spacing between the tubes leads to a cold fluid region to appear in the downstream as seen in the blue region (underworked fluid) for (S ≥ 1), this large spacing permits the ambient (cold) fluid to flow downstream and leads to decrease the heat transfer density since the thermal conductance between the tubes decreased.

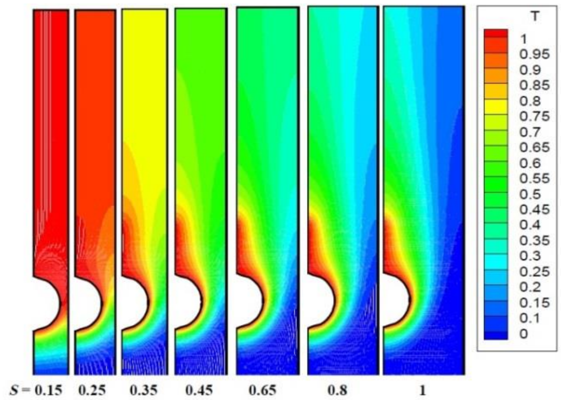

Figure (7) Temperature contour with various spacing between the tube for (Ra=10^3, Pr =0.7, and tube position δ=0.25)

As Rayleigh number increases to (Ra =10^5) same behavior of the temperature contour to that of (Ra =10^3) can be observed in figure (8) except that the optimal spacing here becomes smaller, note that (S_{opt} = 0.35 at Ra=10^3) while (S_{opt} = 0.1 at Ra =10^5), so as Rayleigh number increases the optimal spacing decreases because the thermal boundary layer thickness decreases with increasing of Rayleigh number.

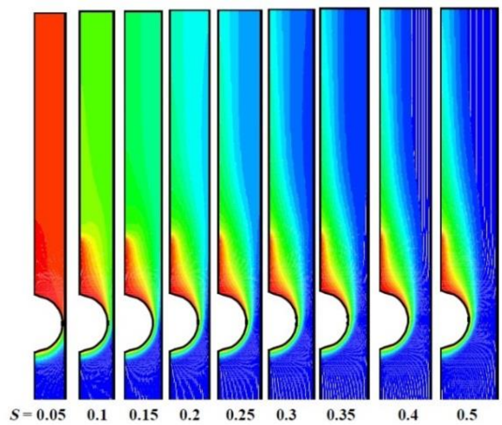

Figure (8) Temperature contour with various spacing between the tube for (Ra=10^5, Pr =0.7, and tube position δ=0.25)

Figures (9, and 10) illustrate the temperature contours at (δ = 0. 5) for Rayleigh numbers (10^3, and 10^5), respectively. In can be seen from both figures that the thermal boundary layer thickness on the lower fin is thinner than the thermal boundary layer on the upper fin due to the presence on the tube in the mid position (δ = 0. 5).

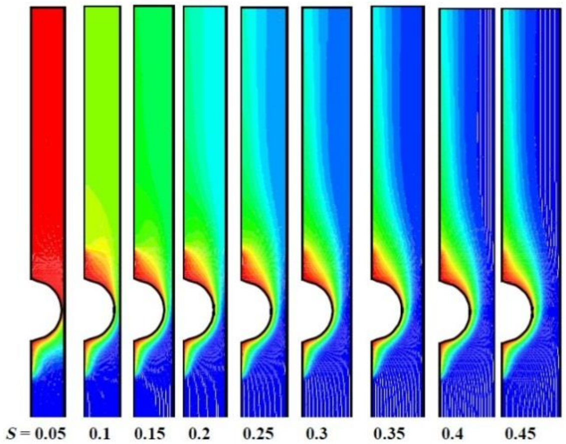

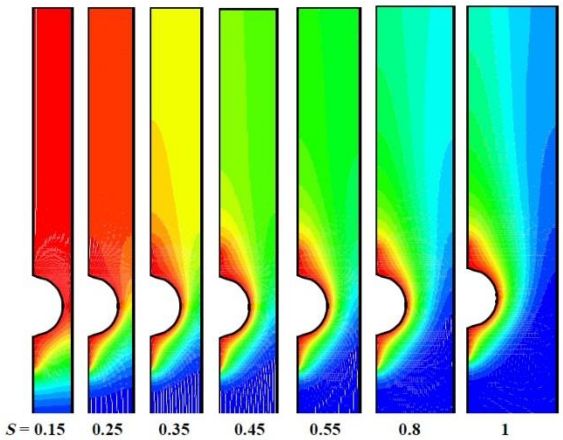

Figure (9) Temperature contour with various spacing between the tube for (Ra=10^3, Pr =0.7, and tube position δ=0.5)

Figure (10) Temperature contour with various spacing between the tube for (Ra=10^5, Pr =0.7, and tube position δ=0.5)

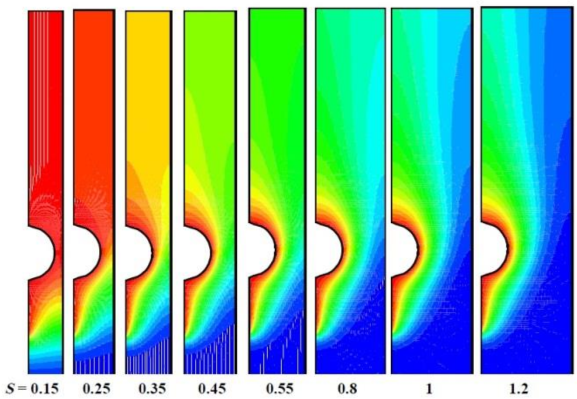

Figure (11) Temperature contour with various spacing between the tube for (Ra=10^3, Pr =0.7, and tube position δ=0.75)

Figures (11, and 12) illustrate the temperature contours at (δ = 0. 75) for Rayleigh numbers (10^3, and 10^5), respectively. It is interesting to note that as the tube moves from the position (δ = 0.25) to the position (δ = 0.75) the thermal boundary layer thickness on the fin surface becomes thicker as shown in figures (11, and 12) in compare with figures (8, and 9).

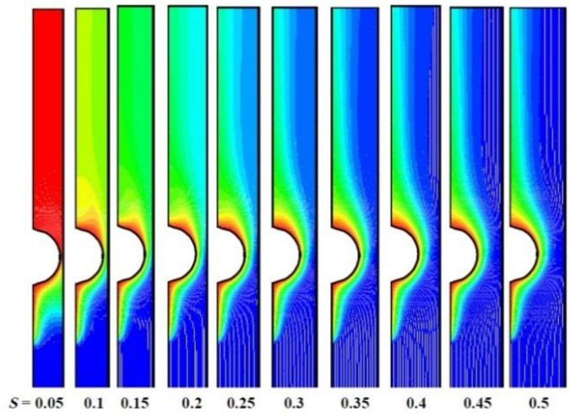

Figure (12) Temperature contour with various spacing between the tube for (Ra=10^5, Pr =0.7, and tube position δ=0.75)

Figures (13 and 14) show the dimensionless heat transfer density as a function of the spacing at different Rayleigh numbers and for tube positions (δ =0.25, and 0.75) respectively. These figures show that there is optimal value of spacing for each Rayleigh number. At this value of spacing the heat transfer density reaches its maximum value (tops of the curves).

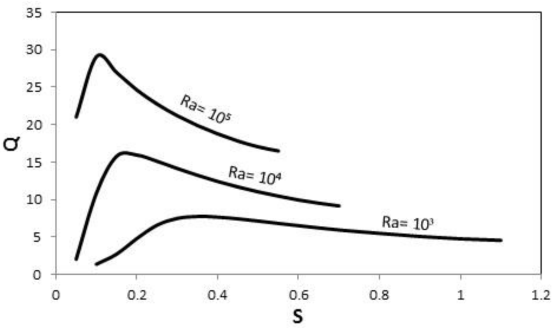

Figure (13) Heat Transfer Density with spacing at different Rayleigh numbers for tube position (δ =0.25)

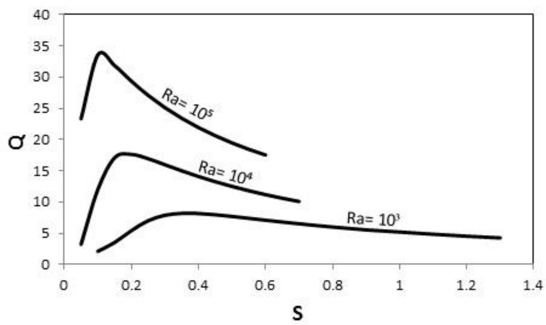

Figure (14) Heat Transfer Density with spacing at different Rayleigh numbers for tube position (δ =0.75)

Figure (15) shows the optimal spacing (S_{opt}) versus Rayleigh number at tube position (δ = 0,25), it is interesting to note that the optimal spacing decreases as Rayleigh number increases, as mentioned above the increasing of Rayleigh number reduces the thermal boundary layer thickness and thus the optimal spacing decreased.

Figure (16) shows the maximum heat transfer density versus Rayleigh number at various tube position (δ), it can be noted that the maximum heat transfer density increases as Rayleigh number increases for all values of (δ), the increasing of Rayleigh number leads to increase the buoyancy force and thus increase the maximum heat transfer density. It also can be seen that at (Ra=10^5) the highest value of the maximum heat transfer density occurs at (δ = 0.75) and the lowest value occurs at (δ =0.25). This can be explained as the tube moves upward to (δ = 0.75) the temperature gradient near the lower fin increases and thus the maximum heat transfer density increases.

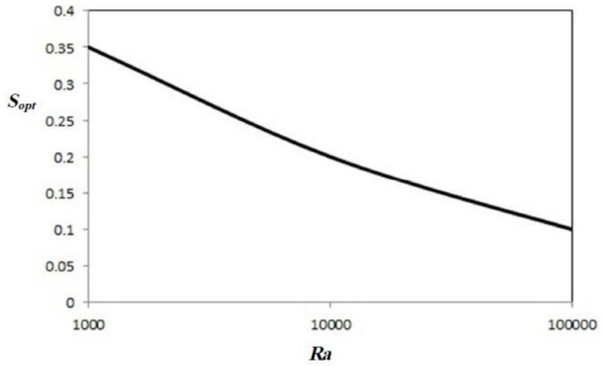

Figure (15) Optimal spacing with Rayleigh number for for tube position (δ =0.25)

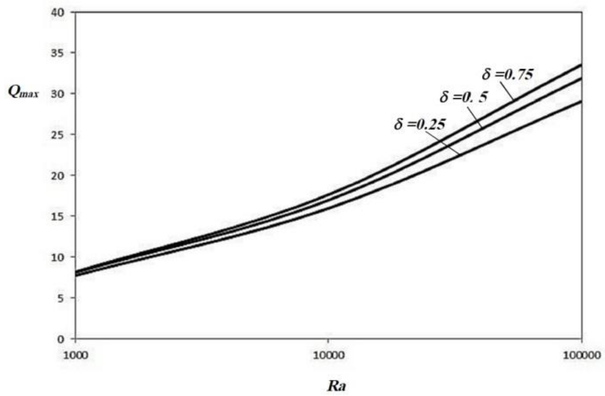

Figure (16) Maximum heat transfer density with Rayleigh number for different axis ratios

Figure (17) shows the optimal spacing versus the tube position of the tube at different Rayleigh numbers. The optimal spacing is constant for all values of the tube position. Since the optimal spacing is constant for all (δ), the number of tubes installed in a fixed volume is the same for all tube positions (δ).

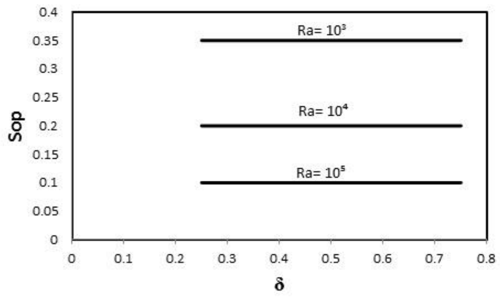

Figure (17) Optimal spacing with tube position for different Rayleigh number

8. Experimental Results:

Figure (18) shows the experimental heat transfer density (Q_{exp}) as a function of the spacing (S) between the tubes for (Ra =3.8×10^4) and for tube position of (δ = 0.667). This figure demonstrates the existence of the optimal spacing (S_{opt}) that maximizes the heat transfer density. The behavior of the experimental curve is similar to the numerical curve of the heat transfer density with spacing which shown in figure (13). The agreement between the experimental and numerical results is qualitative. Table (4) shows the comparison between the experimental optimal spacing and the numerical optimal spacing for Rayleigh number (Ra =3.8×10^4) and tube position (δ= 0.667). The agreement between the experimental and numerical S_{opt} values (within 32 percent) is reasonable in view of the by-pass air flow from the sides of the row. The limitation in the experimental apparatus is the horizontal dimension (L), in the experiment a buoyant air is by-passed on the outside of the elemental channels and this is differing from the numerical model in which assumed that (L>>S) (so that in numerical model the by- pass air from the row sides is negligible). In the view of the mentioned by-pass air the agreement between the experimental and numerical results is good.

Table 4 Comparison between Numerical and Experimental Optimal Spacing (S_{opt}) at Ra =$3.8 \times 10^4$and δ=0.667

S_{opt} (Numerical)	S_{opt} (Experimental)	Error %
0.25	0.37	0.32

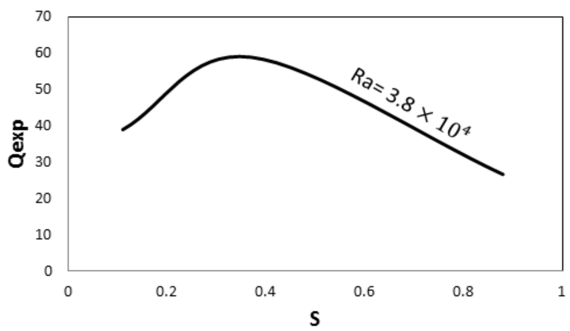

Figure (18) Experimental Heat Transfer Density with spacing at Ra= 3.8×10^4 for tube position (δ =0.667)

9. Conclusions

The conclusions for optimal spacing between finned tubes cooled by free convection can be summarized as:-

1- The optimal spacing decreases as Rayleigh number increases for all tube positions.

2- The maximum heat transfer density increases as Rayleigh number increases for all tube positions.

3- At $Ra=10^5$, the highest value of the maximum heat transfer density occurs at tube position ($\delta = 0.75$) and lowest value occurs at tube position ($\delta = 0.5$).

4- The optimal spacing remains constant as the tube position increases at constant Rayleigh number.

5- The number of finned tubes installed in a fixed volume is the same for all tube positions.

6- The behavior of the experimental heat transfer density (Q_{exp}) and numerical heat transfer density (Q) is qualitative.

10. References

1- Bejan A. and Lorente S., Design with Constructal Theory, Wiley, New York, 2008.

2-Bejan A., Convection Heat Transfer, , Wiley, New York, 1984.

3- Bejan A., Fowler A.J., and Stanescu G., The optimal spacing between horizontal cylinders in a fixed volume cooled by natural convection, International Journal of Heat and Mass Transfer 38, 2047–2055, 1995.

4-Ledezma G. A., and Bejan A., Optimal Geometric Arrangement of Staggered Vertical Plates in Natural Convection, Journal of Heat Transfer, 119, 700-708, 1997.

5- Da Silva A.K., Bejan A., Maximal Heat Transfer Density in Vertical Morphing Channels with Natural Convection, Numerical Heat Transfer, Part A, 45: 135–152, 2004

6- Da Silva A.K., and Bejan A., Constructal multi-scale structure for maximal heat transfer density in natural convection, Int. J. Heat Fluid Flow 26, 34–44, 2005.

7- Da Silva A.K., Lorenzini G., and Bejan A., Distribution of heat sources in vertical open channels with natural convection, International Journal of Heat and Mass Transfer 48, 1462–1469, 2005.

8-Bello-Ochende T., and Bejan A., Constructal multi-scale cylinders with natural convection, International Journal of Heat and Mass Transfer 48, 4300–4306, 2005.

9- Page L., Bello-Ochende T., and Meyer J., Maximum heat transfer density rate enhancement from cylinders rotating in natural convection, Int. Commun. Heat Mass Transfer 38, 1354–1359, 2011.

10- Page L., Bello-Ochende T., and Meyer J., Constructal multi scale cylinders with rotation cooled by natural convection, International Journal of Heat and Mass Transfer 57, 345–355, 2013.

11- Zhang Z., Bejan A., and Lage J.L., Natural Convection in a Vertical Enclosure with Internal Permeable Screen, Journal of Heat Transfer, 113, 377-383, 1991.

12- Rhie, C. M., and Chow, W. L., Numerical Study of the Turbulent Flow Past an Airfoil with Trailing Edge Separation , AIAA Journal, 21, 1525-1532, 1983.